Heat Transfer Engineering, 21:53–61, 2000

0145–7632/00 $12.00 + .00

Developing Laminar Flow and Heat Transfer in Annular-Sector Ducts

M. J. LIN, Q. W. WANG, and W. Q. TAO

School of Energy and Power Engineering, Xi'an Jiaotong University, Xi'an, Shaanxi, People's Republic of China

For annular-sector ducts, steady, laminar, and constant-property forced-convection flow and heat transfer in the entrance region have been analyzed numerically using a general, marching procedure. Two types of thermal boundary conditions have been considered: (1) uniform temperature both axially and peripherally (T boundary condition); (2) uniform axial heat flux with uniform peripherally temperature at any cross section (H1 boundary condition). Numerical analysis has been conducted in the following range of parameters: D_i/D_o *= 0.00, 0.25, 0.50, apex angle of the sector* $2\alpha = 18^\circ, 20^\circ, 24^\circ, 30^\circ, 40^\circ$, *and* $Pr = 0.707$. *The solutions of the developing Nusselt number and friction factor are presented as functions of nondimensional axial distance. Comparisons are made between the computed results and the analytical or numerical results available in the literature. For all cases compared, satisfactory agreement is obtained.*

Internally finned tubes are commonly used as efficient means of augmenting convective heat transfer in tubular heat exchangers. A number of numerical investigations have been performed for the heat transfer and pressure drop characteristics in fully developed regions of various internally finned tubes [1–8]. For laminar developing flow and heat transfer in a circular tube with internal longitudinal fins, numerical simulations have been conducted [9–11] assuming the flow to be parabolic in the axial direction.

In circular and annular tubes with longitudinal fins there are two limiting cases which are widely used in engineering. One is the sector duct, which can be considered as the limiting case of a circular tube with its longitudinal continuous fins spanning the full length of the radius. The other is the annular-sector duct [12], for which the fins in annulus span the full width of the annulus. The numerical analysis of the developing fluid flow and heat transfer in the circular-sector duct was conducted by Lei and Trupp [7] and Chung and Hsia [13]. Although the fully developed fluid flow and heat transfer in the annular-sector duct has been performed by several authors [8, 14–16], no results are provided in the literature for the developing region. The thermally developing laminar flow and heat transfer in ducts of different cross sections continue to be an interesting subject in recent literature [17–19], but the developing situation in the annular-sector duct is still not involved. The annular-sector duct may be considered as one subchannel of a multipassage annular tube, which is used in the intercooler of gas compressors for the cooling of pressurized gas, in double-pipe heat exchangers, etc. The aim of the present study is to predict numerically

This work was supported by the Doctorate Foundation of Chinese Universities and Institutes (No. 9569801). Towards the end of the work, it was also supported by the National Natural Science Foundation of China (No. 59676019).

Address correspondence to Prof. Wen-Quan Tao, School of Energy and Power Engineering, Xi'an Jiaotong University, Xi'an, Shaanxi 710049, People's Republic of China. E-mail: wqtao@xjtu.edu.cn

the developing laminar flow and heat transfer through annular-sector ducts with apex angles ranging from 18° to 40°.

MATHEMATICAL FORMULATION

As shown schematically in Figure 1*a*, the duct being investigated has outer diameter D_o, inner diameter D_i, and an apex angle 2α. The fluid flowing through it is assumed to be incompressible and of constant properties. The flow is laminar and in steady state. Moreover, viscous dissipation and the effect of natural convection in the cross plane are neglected. Considering the symmetry of the problem, only half of the duct should be taken into account, the cross section of which is shown in Figure 1*b*.

The fluid entering the duct has a uniform inlet velocity w_{in} and a uniform temperature T_{in}. As a fundamental research, in the following, two typical thermal boundary conditions will be considered, i.e., isothermal both axially and peripherally (T boundary condition) and uniform heat flux axially with uniform temperature peripherally (H1 boundary condition).

The problem under consideration has a predominant direction (the axial direction) in which upwind convective influence exerts strongly on the downwind flow, so it can be traced to be parabolic in the streamwise direction and the streamwise diffusion of momentum and energy can be omitted.

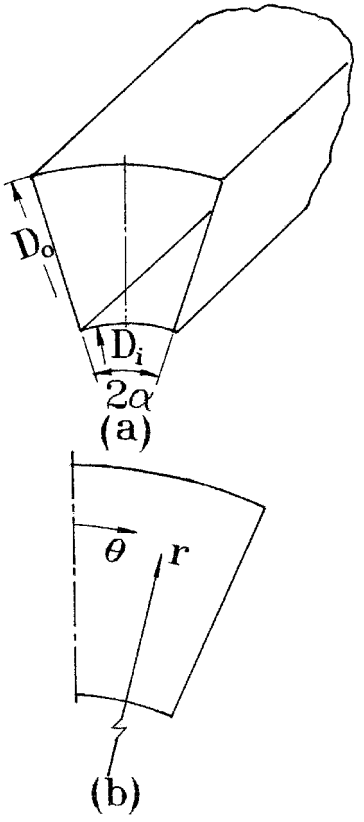

Figure 1 Annular-sector duct: (*a*) pictorial view; (*b*) cross section.

Introduction of the parabolic approximation allows the pressure to be written as

$$p = \bar{p} + \tilde{p} \tag{1}$$

$$\frac{\partial p}{\partial z} = \frac{d\bar{p}}{dz} \qquad \frac{\partial p}{\partial \theta} = \frac{\partial \tilde{p}}{\partial \theta} \qquad \frac{\partial p}{\partial r} = \frac{\partial \tilde{p}}{\partial r} \tag{2}$$

where $\bar{p}$ can be thought as a form of space-averaged pressure over the duct cross section, and $\tilde{p}$ is the small pressure variation governing the flow distribution in the cross-stream plane. Such assumption reveals the uncoupling of longitudinal and lateral pressure gradients, which may be calculated in different way. The velocity component in the main flow direction is driven by the gradients of $\bar{p}$ (i.e., the term $d\bar{p}/dz$), while for the cross-stream flow the gradients of $\tilde{p}$ enter into the momentum equations. As a result, to predict the performance numerically, computations for a three-dimensional parabolic flow are sufficient by employing a marching-type procedure which involves the solution of a two-dimensional elliptic problem in the cross section plane by plane.

Considering the r, θ, z polar-cylindrical coordinates shown in Figure 1, the governing equations for the present problem reduce to the parabolized Navier-Stokes equations devoid of the axial diffusion terms.

By introducing the dimensionless variables $R = 2r/D_h$, $Z = z/(D_h \,\text{Re})$, $U = u/(2\nu D_h)$, $V = v/(2\nu D_h)$, $W = w/w_{\text{in}}$, $P = p/(\rho w_{\text{in}}^2)$, $\text{Re} = w_{\text{in}} D_h/\nu$, $D_h = \pi(D_o^2 - D_i^2)/[\pi D_o + \pi D_i + (D_o - D_i)]$, $\phi_{\text{T}} = (T - T_{\text{in}})/(T_W - T_{\text{in}})$, $\phi_{\text{H1}} = (T - T_{\text{in}})/(Q'/k_f)$, the dimensionless governing equations are as follows:

Continuity:

$$\frac{1}{R}\frac{\partial (RV)}{\partial R} + \frac{1}{R}\frac{\partial U}{\partial \theta} + \frac{\partial W}{\partial Z} = 0 \tag{3}$$

r Momentum:

$$V\frac{\partial V}{\partial R} + \frac{U}{R}\frac{\partial V}{\partial \theta} + W\frac{\partial V}{\partial Z} = -\frac{\partial \tilde{P}}{\partial R} + \frac{1}{R}\frac{\partial}{\partial R}\left(R\frac{\partial V}{\partial R}\right) + \frac{1}{R^2}\frac{\partial^2 V}{\partial \theta^2} + \frac{U^2}{R} - \frac{V}{R^2} - \frac{2}{R^2}\frac{\partial U}{\partial \theta} \tag{4}$$

θ Momentum:

$$V\frac{\partial U}{\partial R} + \frac{U}{R}\frac{\partial U}{\partial \theta} + W\frac{\partial U}{\partial Z} = -\frac{1}{R}\frac{\partial \tilde{P}}{\partial \theta} + \frac{1}{R}\frac{\partial}{\partial R}\left(R\frac{\partial U}{\partial R}\right) + \frac{1}{R^2}\frac{\partial^2 V}{\partial \theta^2} - \frac{UV}{R} - \frac{U}{R^2} + \frac{2}{R^2}\frac{\partial V}{\partial \theta} \quad (5)$$

z Momentum:

$$V\frac{\partial W}{\partial R} + \frac{U}{R}\frac{\partial W}{\partial \theta} + W\frac{\partial W}{\partial Z} = -\frac{d\tilde{P}}{dZ} + \frac{1}{R}\frac{\partial}{\partial R}\left(R\frac{\partial W}{\partial R}\right) + \frac{1}{R^2}\frac{\partial^2 W}{\partial \theta^2} \quad (6)$$

Energy:

$$V\frac{\partial \phi}{\partial R} + \frac{U}{R}\frac{\partial \phi}{\partial \theta} + W\frac{\partial \phi}{\partial Z} = \frac{1}{\mathrm{Pr}}\left[\frac{1}{R}\frac{\partial}{\partial R}\left(R\frac{\partial \phi}{\partial R}\right) + \frac{1}{R^2}\frac{\partial^2 \phi}{\partial \theta^2}\right] \quad (7)$$

The corresponding inlet and boundary conditions are as follows:

At $Z = 0$: $U = 0, V = 0, W = 1$
$\phi_T = 0$ (for T condition),
$\phi_{H1} = 0$ (for H1 condition)
At wall surfaces: $U = 0, V = 0, W = 0$
$\phi_T = 1$ (for T condition)
$\phi_{H1} = \phi(Z)$ (for H1 condition)

COMPUTATIONAL PROCEDURE

Using the control-volume-based, fully implicit, finite-difference method, the procedure used in the present study is basically the same as proposed by Patankar and Spalding [20], except that the discretization scheme for the convection-diffusion terms in the cross section is the power-law scheme. The details of solution procedure can be found in [20].

It should be noted that for the case of isothermal condition, solving the energy equation is quite straightforward. However, for the H1 boundary condition, only a uniform axial heat input is given, while the temperature $T_W(z)$ is unknown beforehand and is a function of z. Prakash and Liu [9] recommended a procedure in which the wall temperature for the downstream cross section is adjusted iteratively until the computed bulk temperature $T_b(z)$ agrees with the exact bulk temperature obtained by a heat balance. This method was adopted in the present study.

Numerical computations were performed in the following parameter ranges: $\mathrm{Pr} = 0.707$, $2\alpha = 18°$, 20°, 24°, 30°, 40°, and $D_i/D_o = 0.00, 0.25, 0.50$.

In order to get better resolution of the developing process, the step size of the marching procedure was gradually increased, and it was determined as follows: $\Delta z(k) = (z/125{,}000)\cdot(1.1)^{k-1}$, where $\Delta z(k)$ is the marching step size advanced from the kth cross section to the $(k+1)$th cross section. For the case of $2\alpha = 18°$, $\mathrm{Pr} = 0.707$, and $D_i/D_o = 0.25$, two grid systems were used in exploratory runs: $16(r) \times 25(\theta) \times 90(z)$ and $32(r) \times 50(\theta) \times 90(z)$. It was found that the differences in the overall results of friction factor and Nusselt number was around 1%. The accuracy of the numerical solution from the $16 \times 25 \times 90$ grids was deemed satisfactory, hence this grid system was used for all computations.

At each marching step, the convergence criterion of iteration process was that the relative change in ϕ of successive two iterations was less than 5×10^{-5}. The number of iterations needed was usually about 200.

Numerical results were obtained for both the developing and the fully developed regions of each duct. The fully developed results were obtained first by solving a 2D elliptic problem. Then, the results in the developing region were computed step by step along the axial direction. The entire length calculated was 200 times D_h. It usually took 45 steps to make the local friction factor and Nusselt number approach their corresponding fully developed values within 1% difference. In the following, the numerical results will be presented in three separate parts, the hydrodynamic results first, then the thermal results for the H1 boundary condition, and finally the results for the T boundary condition.

HYDRODYNAMIC RESULTS

It is convenient to present the pressure drop results in terms of a friction factor f_h, defined as

$$f_h = \frac{(-d\bar{p}/dz)\cdot D_h}{(\rho \bar{w}_{\mathrm{in}})^2/2} \qquad \mathrm{Re}_h = \frac{w_{\mathrm{in}}\cdot D_h}{\nu} \quad (8)$$

The pressure drop from the inlet to some given axial location downstream may be expressed in the following manner:

$$\frac{\bar{p}_{\mathrm{in}} - \bar{p}(z)}{(\rho w_{\mathrm{in}}^2/2)} = (f_{\mathrm{fd},h}\cdot \mathrm{Re}_h)\left(\frac{z}{D_h\cdot \mathrm{Re}_h}\right) + K(z) \quad (9)$$

Table 1 Hydrodynamic numerical results

D_i/D_o	Result	18°	20°	24°	30°	40°
0.00	$f_{\mathrm{fd},h}\cdot \mathrm{Re}_h$	50.663	51.027	51.712	52.652	54.034
	$K(\infty)$	1.959	1.922	1.865	1.792	1.698
	$L_{\mathrm{hy}}/(D_h\cdot \mathrm{Re}_h)$	0.129	0.128	0.124	0.101	0.0952
0.25	$f_{\mathrm{fd},h}\cdot \mathrm{Re}_h$	63.224	62.724	61.806	60.630	59.182
	$K(\infty)$	1.672	1.670	1.607	1.565	1.521
	$L_{\mathrm{hy}}/(D_h\cdot \mathrm{Re}_h)$	0.0909	0.0911	0.091	0.0838	0.0771
0.50	$f_{\mathrm{fd},h}\cdot \mathrm{Re}_h$	61.847	60.723	59.033	57.599	57.078
	$K(\infty)$	1.396	1.425	1.460	1.498	1.246
	$L_{\mathrm{hy}}/(D_h\cdot \mathrm{Re}_h)$	0.0728	0.0747	0.0781	0.0762	0.0594

where $f_{\mathrm{fd},h}$ is the fully developed friction factor, and $K(z)$ is the dimensionless excess pressure drop (or the incremental pressure drop) due to entrance effect. Once the axial location was sufficiently far from the inlet, the value of $K(z)$ reduced to a constant $K(\infty)$. The numerical results of hydrodynamic computation will be presented in the form of f_h and $K(\infty)$ as a function of z.

Value of f ·Re

The fully developed values of $f_{\mathrm{fd},h}\cdot \mathrm{Re}_h$ obtained in the present study are given in Table 1. The agreement of the present numerical results with the previous analytical solutions for the annular-sector duct [21] and with the circular-sector duct [22] is quite satisfactory. For example, the numerical results of $f_{\mathrm{fd},h}\cdot \mathrm{Re}_h$ for $2\alpha = 20°$, $D_i/D_o = 0.50$ differs from the analytical one by only 0.78%.

The variation of $f_h\cdot \mathrm{Re}_h$ in the entrance region is presented in Figure 2. As expected, the axial distribution of $f_h\cdot \mathrm{Re}_h$ for all ducts studied demonstrates a common trend: decreasing with $z/(D_h\cdot \mathrm{Re}_h)$ sharply at first, then tending to level off and approaching the fully developed value asymptotically.

Variation of Incremental Pressure Drop

Variation of the incremental pressure drop in the entrance region is presented in Figure 3. As expected, $K(z)$ increases with z, approaching asymptotically a constant value at certain large axial distance. This behavior is entirely consistent with the interpretation of $K(z)$ as the accumulated increment in the pressure drop due to flow development between $z = 0$ and z. The asymptotical value that $K(z)$ approaches for large z is called $K(\infty)$, which corresponds to the overall incremental pressure drop due to entry flow development process.

As a check of our code, a preliminary computation was performed for a circular tube. The numerical result of $K(\infty)$ is 1.247, which agrees with Bender's theoretical result [23] (1.25) very well.

The values of $K(\infty)$ are also summarized in Table 1. Results of the table indicate that for a given value of D_i/D_o, the $K(\infty)$ increases with the decrease in apex angle 2α. For a given apex angle 2α, the values of $K(\infty)$ decreases with the increase in D_i/D_o.

For the circular sector duct ($D_i/D_o = 0.0$), Sparrow and Haji-Sheikh [24] obtained $K(\infty) = 1.657$, 2.0, and 2.235, corresponding to $2\alpha = 45°$, 20°, and 15°, respectively. Our numerical results [1.647 (45°), 1.922 (20°), and 2.214 (15°)] agree with Sparrow and Haji-Sheikh's solution very closely. The difference may be partly attributed to the approximation introduced in Sparrow and Haji-Sheikh's analysis, in which the effect of secondary flow in the cross-stream plane was omitted.

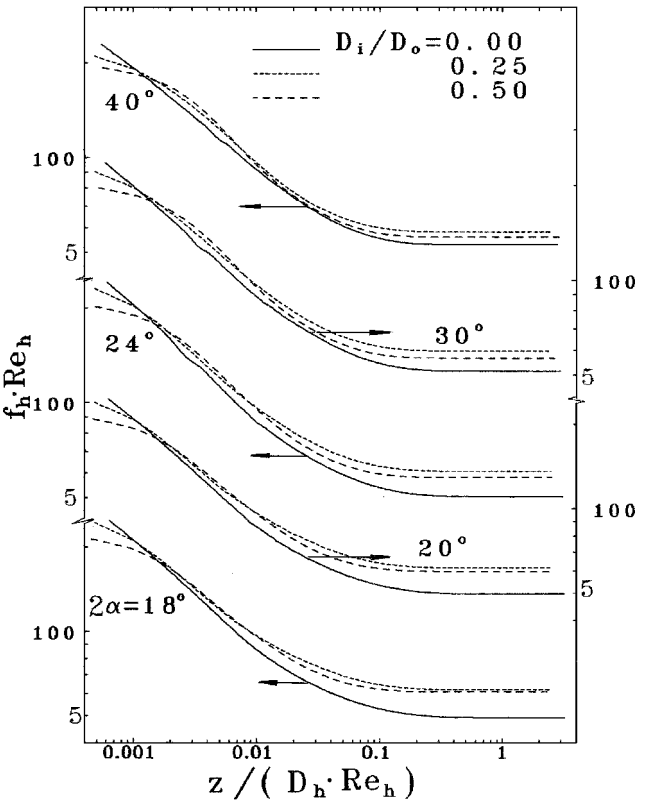

Figure 2 Axial distribution of $f\cdot \mathrm{Re}$.

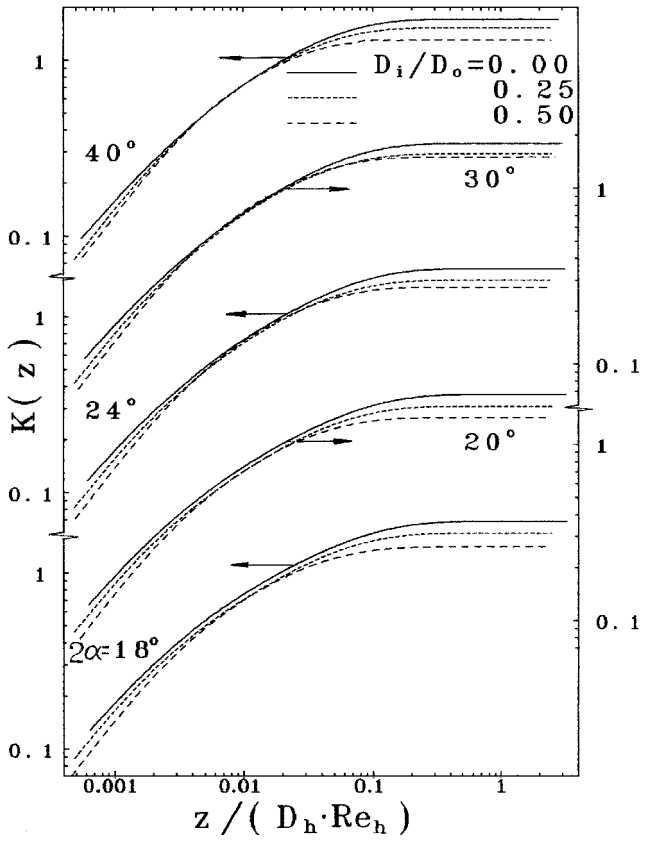

Figure 3 Axial distribution of $K(z)$.

Estimation of the Hydrodynamic Entrance Length

Conventionally [25], the hydrodynamic entrance length L_{hy} is defined as the distance for the axial velocity at the center line to reach 99% of the fully developed value. This length may also be defined in terms of the distance required for $K(z)$ to approach its fully developed value within a preassigned percentage (i.e., 99%) [26].

According to the first definition, Prakash and Liu [9] have gained values of $L_{hy}/(D_h \cdot \mathrm{Re}_h) = 0.054$ for a circular duct. Using a linearized analysis, Hornbeck [27] obtained $L_{hy}/(D_h \cdot \mathrm{Re}_h) = 0.056$. For the same configuration, the present computations attained $L_{hy}/(D_h \cdot \mathrm{Re}_h) = 0.0538$ using the first definition and 0.0547 according to the second definition. To estimate the hydrodynamic entrance length of the annular-sector ducts, the authors adopted the second definition. Numerical results of L_{hy} from the second definition are also presented in Table 1.

Following features may be noted from this table. (1) For the circular-sector duct, the apex angle has a monotonic effect on the hydrodynamic entrance length, i.e., L_{hy} increases with a decrease in α. (2) For the annular-sector ducts, the effect of α on L_{hy} exhibits a bit more complicated behavior. From $2\alpha = 18°$ to 24°, L_{hy} increases slightly with increase in α, while further increase in α leads to an appreciable decrease in L_{hy}. (3) With an increase in D_i/D_o, L_{hy} decreases quite significantly. (4) For all the cases studied, the values of $L_{hy}/(D_h \cdot \mathrm{Re}_h)$ are higher than those of the circular tube. Probably, the irregularity in cross-section geometry retards the developing process of the velocity field.

THERMAL RESULTS OF H1 BOUNDARY CONDITION

For this type of thermal boundary condition, the bulk temperature of the fluid at any axial location $T_b(z)$ can be obtained by a heat balance as

$$T_b(z) = T_{in} + \frac{Q'z}{\dot{m}C_p} \tag{10}$$

The local Nusselt number can be defined as

$$\mathrm{Nu}_{h,H1}(z) = \frac{Q'/[\alpha(D_i + D_o) + (D_o - D_i)]}{T_w(z) - T_b(z)} \cdot \frac{D_h}{k_f} \tag{11}$$

Nusselt Number for Fully Developed Flow

The numerical results of Nu_{H1} are presented in Table 2. The agreement between our numerical and analytical results [8, 15] is quite satisfactory. For example, for $2\alpha = 20°$, $D_i/D_o = 0.25$, the numerical value of Nu_{H1} equals 3.848, which differs with the solution of [15] by 2.5%. The deviation of other cases is usually smaller.

Local Nusselt Number in the Entrance Region

The variation of the local Nusselt number is displayed in Figure 4. As expected, the Nusselt number is very large at the beginning of the entrance. It decreases with increasing axial distance, approaching the fully developed value asymptotically.

Estimate of the Thermal Entrance Length

The thermal entrance length L_{H1} is usually defined as the length required for the local Nusselt number to equal 1.05 times its fully developed value [25]. Here, the present authors adopt another definition. It is well known that for the H1 boundary condition, both the duct-wall temperature $T_W(z)$ and the bulk temperature $T_b(z)$ are functions of z. The difference between $T_W(z)$

Table 2 Thermal numerical results

D_i/D_o	Results	18°	20°	24°	30°	40°
0.00	$Nu_{fd,T}$	2.029	2.117	2.304	2.383	2.622
	$L_T/(D_h \cdot Re_h)$	0.129	0.115	0.104	0.0877	0.0778
	$Nu_{fd,H1}$	2.796	2.852	2.954	3.089	3.278
	$L_{H1}/(D_h \cdot Re_h)$	0.0932	0.0845	0.0754	0.0609	0.0483
0.25	$Nu_{fd,T}$	2.897	2.868	3.091	3.162	3.185
	$L_T/(D_h \cdot Re_h)$	0.0937	0.0888	0.085	0.0758	0.0556
	$Nu_{fd,H1}$	3.829	3.838	3.848	3.846	3.823
	$L_{H1}/(D_h \cdot Re_h)$	0.0652	0.0600	0.0506	0.0464	0.0389
0.50	$Nu_{fd,T}$	3.572	3.558	3.327	3.246	3.232
	$L_T/(D_h \cdot Re_h)$	0.106	0.0919	0.0744	0.0629	0.0481
	$Nu_{fd,H1}$	4.138	4.042	3.894	3.863	3.851
	$L_{H1}/(D_h \cdot Re_h)$	0.0367	0.0360	0.0348	0.0344	0.0301

and $T_b(z)$ decreases with the development of heat transfer, ultimately taking a constant value characteristic of fully developed heat transfer. Such a tendency is very like that of $K(z)$. Therefore, we can naturally define the thermal entrance length in terms of the distance required for $T_W(z) - T_b(z)$ to approach its fully developed value within a preassigned percentage (i.e., 95%). This definition is consistent with the definition of hydrodynamic entrance length discussed earlier. Table 2 lists the estimated thermal entrance length for the H1 boundary condition. The value of $L_{H1}/(D_h \cdot Re_h)$ decreases with increase in α and (or) D_i/D_o.

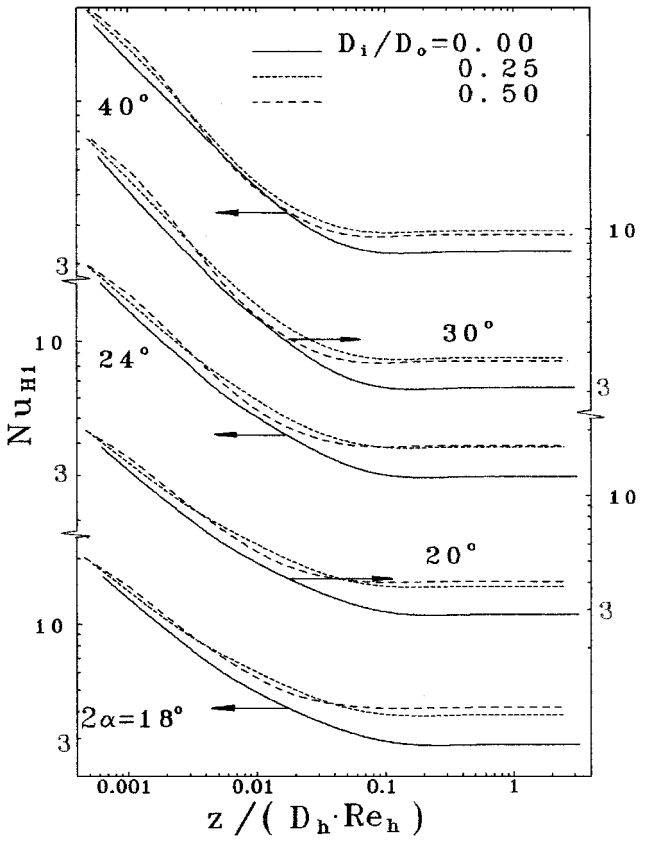

Figure 4 Axial distribution of Nu_{H1}.

THERMAL RESULTS OF THE T BOUNDARY CONDITION

The bulk temperature $T_b(z)$ at any axial location z is given as

$$T_b(z) = \frac{1}{\dot{m}C_p}\int_A C_p \rho w T \, dA \tag{12}$$

the total heat transfer rate $Q(z)$ up to a distance z is equal to

$$Q(z) = \dot{m}C_p[T_b(z) - T_{in}] \tag{13}$$

Defining the log-mean temperature difference ΔT_{lm} as

$$\Delta T_{lm}(z) = \frac{(T_w - T_{in}) - [T_w - T_b(z)]}{\ln\{(T_w - T_{in})/[T_w - T_b(z)]\}} \tag{14}$$

The average Nusselt number up to the axial location z can be defined as

$$\bar{Nu}_{h,T}(z) = \frac{Q(z)/\{[\alpha(D_i + D_o) + (D_o - D_i)]z\}}{\Delta T_{lm}(z)} \cdot \frac{D_h}{k_f} \tag{15}$$

where the overbar represents average. The subscript h designates that D_h is used as the characteristic length and the subscript T identifies the T boundary condition.

Let $dQ(z)/dz$ be the rate of increase of $Q(z)$ with the axial distance. Defining the local log-mean temperature difference:

$$\Delta T_{lm}(k) = \frac{[T_w - T_b(k-1)] - [T_w - T_b(k)]}{\ln\{[T_w - T_b(k-1)]/[T_w - T_b(k)]\}} \tag{16}$$

The local Nusselt number can be defined as

$$\bar{\mathrm{Nu}}_{h,\mathrm{T}}(k) = \frac{[dQ(z)/dz]/[\alpha(D_i + D_o) + (D_o - D_i)]}{\Delta T_{\mathrm{lm}}(k)} \cdot \frac{D_h}{k_f} \tag{17}$$

Fully Developed Nusselt Number

The fully developed Nusselt numbers are presented in Table 2. For $D_i/D_o = 0.25$, 0.50, the fully developed Nusselt numbers of the T boundary condition were solved by Ben-Ali et al. [8]. Our numerical results agree with Ben-Ali et al.'s within 2%.

Variation of the Local Nusselt Number

Variation of the local average Nusselt number along the axis is presented in Figure 5. As expected, the Nusselt number is large near the inlet, and decreases asymptotically to the fully developed value. With the increases in apex angle, the difference in fully developed Nusselt number for different D_i/D_o decreases.

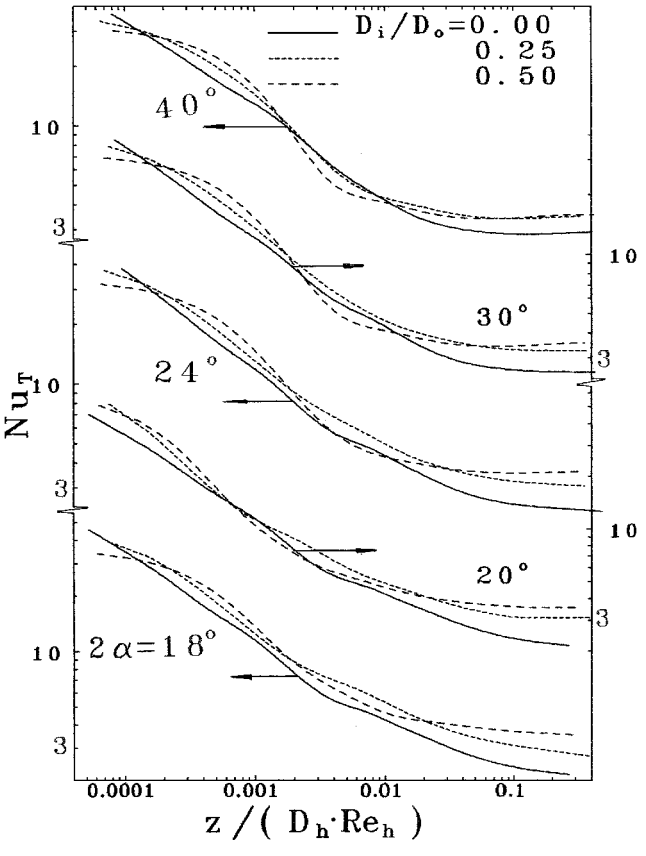

Figure 5 Axial distribution of Nu_{T}.

Estimation of the Thermal Entrance Length

Estimation of values of the thermal entrance length L_{T}, defined as the distance required for the local Nusselt number to drop to 1.05 times fully developed value, are presented in Table 2. It can be found that with increase in apex angle, the thermal entrance length decreases. While the table shows a mixed dependence of L_{T} on D_i/D_o, which may increase or decrease the strength of the second flow, and the distance required for this flow to decay.

By carefully inspecting Tables 1 and 2, we can find that for all the cases studied, the three entrance lengths, i.e., L_{hy}, L_{H1}, L_{T}, have the following common relation: $L_{\mathrm{H1}} < L_{\mathrm{T}} < L_{\mathrm{hy}}$. This observation is quite consistent with the well-known results obtained for a circular tube. As claimed in many heat transfer textbooks, such as [28], if $\mathrm{Pr} < 1$ the thermal boundary layer in internal flow develops more rapidly than the hydrodynamic boundary layer. Another important finding is that except for the case of $D_i/D_o = 0.5$ and H1 boundary condition, the thermal entrance length for the cases studied is higher than that of a circular tube, for which the value of $L/(D_h \cdot \mathrm{Re}_h)$ for air is about 0.035 [28].

The largest value (0.129) occurs for the case of $D_i/D_o = 0.0$ and with T boundary condition. This finding is of general importance for designing an experimental apparatus to investigate laminar developing flow in a noncircular duct.

CONCLUSIONS

Both hydrodynamically and thermally developing flow and heat transfer of air in annular-sector ducts with H1 and T boundary conditions are investigated numerically by using a marching procedure. The axial distributions of friction factor, local Nusselt number, and the hydrodynamic and thermal entrance lengths are presented. The computed Nusselt number and friction factor agree well with the available solutions in the literature. The major findings may be summarized as follows:

1. Generally speaking, both the hydrodynamic entrance length and the thermal entrance length decrease with the increases in apex angle 2α and the ratio of D_i/D_o. Some exceptional cases may be found, but they do not violate this general rule significantly.
2. For the same geometric configuration, the following general relationship holds: $L_{\mathrm{H1}} < L_{\mathrm{T}} < L_{\mathrm{hy}}$, which implies that for the cases studied, the thermal boundary layer develops more rapidly than the hydrodynamic boundary layer.

3. For most of the cases studied, both the hydrodynamic entrance length (L_{hy}) and the thermal entrance length (L_{H1} and L_T) are higher than that of their counterparts in a circular tube, exhibiting the retarding effect of geometric irregularity on the developing process.

NOMENCLATURE

A	cross-sectional area
C_p	specific heat of fluid
D	diameter of annular duct
D_h	equivalent hydrodynamic diameter
f	friction factor
k	marching step index
k_f	thermal conductivity of fluid
K	incremental pressure drop
L	entrance length (hydrodynamic or thermal)
$\dot{m}$	mass flow rate through duct
Nu	Nusselt number
p	pressure
P	dimensionless pressure
Pr	Prandtl number
Q	total heat transfer up to z
Q'	heat input per unit axial length for the H1 boundary condition
r	radial coordinate
R	dimensionless radius
Re	Reynolds number
T	temperature
T_W	uniform duct and fin temperature for the T boundary condition; local duct and fin temperature at any cross section for the H1 boundary condition.
T_b	mean or bulk temperature at any axial location
u, v, w	angular, radial, and axial velocity components
U, V, W	dimensionless angular, radial, and axial velocity components
z	axial distance; axial coordinate
Z	dimensionless axial coordinate
α	half of apex angle
ΔT_{lm}	log-mean temperature difference
θ	angular coordinate
μ	coefficient of viscosity of the fluid
ν	kinematic viscosity
ρ	density of fluid
ϕ	dimensionless temperature

Superscripts

$\bar{}$	average value
$\tilde{}$	driving pressure in the cross-stream flow

Subscripts

fd	fully developed condition
H1	H1 boundary condition
hy	hydrodynamic results
h	based on the equivalent hydraulic diameter D_h
in	values at the inlet locations
i	inner
o	outer
T	T boundary condition

REFERENCES

[1] Soliman, H. M., and Feingold, A., Analysis of Fully Developed Laminar Flow and Heat Transfer in Internally Finned Tubes, *Chem. Eng. J.*, vol. 14, no. 2, pp. 119–128, 1977.

[2] Soliman, H. M., and Feinglod, A., Analysis of Heat Transfer in Internally Finned Tubes under Laminar Flow Conditions, Proc. 6th Int. Heat Transfer Conf., Toronto, Canada, vol. 2, pp. 571–576, 1978.

[3] Patankar, S. V., Ivanovic, M., and Sparrow, E. M., Analysis of Turbulent Flow and Heat Transfer in Internally Finned Tubes and Annuli, *ASME J. Heat Transfer*, vol. 101, no. 1, pp. 29–37, 1979.

[4] Soliman, H. M., Chau, T. S., and Trupp, A. C., Analysis of Laminar Heat Transfer in Internally Finned Tubes with Uniform Outside Wall Temperature, *ASME J. Heat Transfer*, vol. 102, no. 4, pp. 598–604, 1980.

[5] Trupp, A. C., and Lau, A. C., Fully Developed Laminar Heat Transfer in Circular Sector Ducts with Isothermal Walls, *ASME J. Heat Transfer*, vol. 106, no. 2, pp. 467–469, 1984.

[6] Tao, W. Q., Conjugated Laminar Forced Convective Heat Transfer from Internally Finned Tube, *ASME J. Heat Transfer*, vol. 109, no. 3, pp. 791–795, 1987.

[7] Lei, Q. M., and Trupp, A. C., Further Analysis of Laminar Flow Heat Transfer in Circular Sector Ducts, *ASME J. Heat Transfer*, vol. 111, no. 4, pp. 1088–1090, 1989.

[8] Ben-Ali, T. M., Soliman, H. M., and Zaiffeh, E. K., Further Result for Laminar Heat Transfer in Annular Sector and Circular Ducts, *ASME J. Heat Transfer*, vol. 111, no. 4, pp. 1090–1093, 1989.

[9] Prakash, C., and Liu, Ye-Di, Analysis of Laminar Flow and Heat Transfer of an Internally Finned Circular Duct, *ASME J. Heat Transfer*, vol. 107, no. 1, pp. 84–91, 1985.

[10] Rustman, I. M., and Soliman, H. M., Numerical Analysis of Laminar Forced Convection in the Entrance Region of Tubes with Longitudinal Internal Fins, *ASME J. Heat Transfer*, vol. 110, no. 2, pp. 310–313, 1988.

[11] Kelkar, K. M., and Patankar, S. V., Numerical Prediction of Fluid Flow and Heat Transfer in a Circular Tube with Longitudinal Fins Interrupted in the Streamwise Direction, *ASME J. Heat Transfer*, vol. 112, no. 2, pp. 342–348, 1990.

[12] Carnavos, T. C., Cooling Air in Turbulent Flow with Internally Finned Tubes, *Heat Transfer Eng.*, vol. 1, no. 2, pp. 41–46, 1979.

[13] Chung, B. T. F., and Hsia, R. P., Laminar Flow Developing Heat Transfer in Circular Sector Ducts with H1 and H2 Boundary Conditions, *Heat Transfer Eng.*, vol. 15, no. 4, pp. 55–65, 1994.

[14] Nida, T., Analytical Solution for the Velocity Distribution in Laminar Flow in an Annular-Sector Duct, *Int. Chem. Eng.*, vol. 20, no. 2, pp. 258–265, 1980.
[15] Soliman, H. M., Laminar Heat Transfer in Annular Sector Ducts, *ASME J. Heat Transfer*, vol. 109, no. 1, pp. 247–249, 1987.
[16] Helmut, F. B., Mass Transportation in Circular Sector and Annular Sector Tubes, *Int. J. Heat Mass Transfer*, vol. 31, no. 7, pp. 1451–1469, 1988.
[17] Hsieh, S. S., and Wen, M. Y., Developing Three-Dimensional Laminar Mixed Convection in a Circular Tube Inserted with Longitudinal Strips, *Int. J. Heat Mass Transfer*, vol. 39, no. 2, pp. 299–310, 1996.
[18] Uzun, I., and Unsal, M., A Numerical Study of Laminar Heat Convection in Ducts of Irregular Cross-Sections, *Int. Commun. Heat Mass Transfer*, vol. 24, no. 6, pp. 835–848, 1997.
[19] Lin, C. X., Zhang, P., and Ebadian, M. A., Laminar Forced Convection in the Entrance Region of Helical Pipes, *Int. J. Heat Mass Transfer*, vol. 40, no. 14, pp. 3293–3304, 1997.
[20] Patankar, S. V., and Spalding, D. B., A Calculation Procedure for Heat, Mass and Momentum Transfer in 3-D Parabolic Flows, *Int. J. Heat Mass Transfer*, vol. 15, no. 10, pp. 1787–1806, 1972.
[21] Sparrow, E. M., Chen, T. S., and Tonsson, V. K., Laminar Flow and Pressure Drop in Internally Finned Annular Ducts, *Int. J. Heat Mass Transfer*, vol. 7, no. 5, pp. 583–585, 1964.
[22] Chiranjivi, C., and Vidyanidhi, V., Heat Transfer in Wedge-Shape Ducts, *Indian Chem. Eng.*, vol. 15, no. 1, pp. 49–51, 1973.
[23] Bender, E., Druckverlust bei Laminarer Stromung in Rohreinalauf, *Chem.-Ing.-Tech.*, vol. 41, no. 10, pp. 682–686, 1969.
[24] Sparrow, E. M., and Haji-Sheikh, A., Laminar Heat Transfer and Pressure Drop in Isosceles Triangular, Right Triangular and Circular-Sector Ducts, *ASME J. Heat Transfer*, vol. 87, no. 3, pp. 426–427, 1965.
[25] Shah, R. K., and London, A. L., *Laminar Flow Forced Convection in Ducts*, Academic Press, New York, 1978.
[26] Beavers, G. S., Sparrow, E. M., and Magnuson, R. B., Experiments on Hydrodynamic Developing Flow in Rectangular Tubes, *Int. J. Heat Mass Transfer*, vol. 13, no. 4, pp. 689–675, 1970.
[27] Hornbeck, R. W., Laminar Flow in the Entrance Region of a Pipe, *Appl. Sci. Res.*, *A*, vol. 13, pp. 224–232, 1964.
[28] Incropera, F. P., and DeWitt, D. P., *Introduction to Heat Transfer*, 3d ed., Wiley, p. 411, New York, 1996.

Wen-Quan Tao received his undergraduate diploma (1962) in power machinery engineering and graduate diploma (1966) in heat transfer from Xi'an Jiaotong University, China. He then joined the faculty of the university. From 1980 to 1982, he was a visiting scholar at the Heat Transfer Lab of the Department of Mechanical Engineering of the University of Minnesota (USA). Currently he is a Professor and Dean of the School of Energy and Power Engineering of Xi'an Jiaotong University. He has published more than 100 technical articles in both numerical and experimental heat transfer. He is also the author or co-author of seven books, including a graduate textbook, *Numerical Heat Transfer* (in Chinese).

Mingjie Lin is currently a graduate student in the Computer Engineering Department at Clemson University, SC. He conducted this study when he was a graduate student at Xi'an Jiaotong University (XJTU), China. He holds a Bachelor of Engineering in Mechanical Engineering from XJTU, and a Master's Degree from the Mechanical Engineering Department at Clemson University. His present research activity is related to parallel computational fluid dynamics in multiple processors and distributing computer system.

Qiu-Wang Wang is currently an Associate Professor at the School of Energy and Power Engineering of XJTU. He received his Bachelor of Engineering in Mechanical Engineering in 1991, and his Ph.D. in Engineering Thermophysics in 1996 from XJTU. His research interests include numerical heat transfer, natural heat transfer in enclosures, and convective heat transfer enhancement. He is working in the division of Building Science and Technology at City University of Hong Kong as a visiting scholar.